Investigation of Mixed Convective Stagnated Flow of Casson Nanofluid Past an Exponentially Stretching Sheet, using the Darcy - Forchheimer Model

Rekha Devi[1], Shilpa Sood[1]

Department of Mathematics and Statistics, Career Point University, Hamirpur (Himachal Pradesh), India

Abstract: *This research uses the Darcy-Forchheimer model to analyze steady magneto hydrodynamics (MHD) boundary layer flow with mass and heat transport of Casson nanofluid over an exponentially stretched sheet in a porous medium with mixed convection. Additionally, consideration is given to how the transfer of the heat and the concentration of nanoparticles have been impacted by Brownian motion and thermophoresis. A method known as similarity transformation may be used to translate controlling partial differential equations into ordinary differential equations. The mathematical system of equations is solved by utilizing an inbuilt solver of MATLAB. Investigations have been done into how dimensionless parameters affect flow, heat transmission, and nanoparticle concentration. To investigate many dimensionless parameters impacts on concentration, velocity, and temperature, graphs were plotted and explained.*

Keywords: Brownian motion; casson nanofluid, magneto hydrodynamics; bvp4c solver

1. Introduction

Sadeghy et al. [3] have quantitatively reported the stagnation point flow of an upper convected Maxwell fluid. Ishak et al.[4] investigated an incompressible viscous fluid flow to the vertical porous stretched sheet at the mixed convection stagnation point.

There are numerous industrial operations where magnetic fields are used, including pumping, heating, levitating, and stirring liquid metals [5]. MHD is the research of the movement of fluid which is electrically conducted under the magnetic field effect.

The electrically conducting liquid movement, which produces some mechanical forces and alters the fluid flow, is what produces electric current [6]. An investigation into the effect that magnetic fields have on the flow of blood was carried out by Sud et al. [7], who found that the moving magnetic field caused an increase in the speed at which blood moved. Uddin et al. [8] conducted an experiment to study the natural convective heat-transferring process in a square jar that was filled with the nanofluid and had a waved upper surface.

The process of transferring heat known as 'mixed convection' combines the processes of 'forced convection' with 'natural convection.' Mixed convection flow can essentially be divided into helpful flow and opposing flow, and this categorization is largely predicated on the direction in that the external & buoyancy-induced flow are moving. The heat transmission is supposed to be improved by assisting flow and decreased by opposing flow. Numerous applications, including air nuclear collectors, boundary layer flows, exchangers of heat, solar collectors, and others, use the stagnation-point fluid flow resulting from mixed convection [9,10,11].

Ibrahim and Makinde [12]used the power-law nanofluid to examine the effects of convective heating, velocity slip, "thermophoresis, and Brownian motion on the MHD stagnation point flow. Khan et al. [13]explored oblique hydromagnetic flow having temperature-variable viscosity towards the stagnation point employing MHD Newtonian nanofluid including thermal radiation effects.

The consequences of slip and convective boundary conditions on the MHD stagnation point flow" including the transferring of the heat for the Casson nanofluid were presented by Makinde and Ibrahim [14]and Makinde et al. [15]in their studies. The nanofluid flow containing the phenomena of buoyant force, thermophoresis, "convective heating, Brownian motion, and MHD towards the stagnation point having the impacts of heat has been investigated by Makinde et al. [16].

In the viscous fluid's boundary layer flow encouraged through an inclined stretching sheet, Haung et al.'s study [17]investigated the heat transfer analysis. Qasim et al.[18]conducted research to explore the thermal radiation impacts on the effects of mixed convection flow of viscoelastic fluid along a sheet which is inclined. Sravanthi [19] looked into the MHD slip flow on an exponentially stretched inclined sheet utilizing the Soret-Dufour phenomena. According to Eldahad and Aziz [20], mixed convection, absorption/heat generation, and suction/blowing all had an impact on the MHD boundary layer flow over an inclined stretched sheet.

Soret, magnetic field, Dufour, Joule heating, slip effects, chemical reaction, and Kumar et al.'s [21] investigation of mass and heat transportation on exponentially angled stretching sheets surrounded in porous medium"; The analysis of mass &heat transport in the boundary layers carried out by Keller & Magyari [22] across an exponentially stretched continuous sheet; and many studies addressing

Newtonian & non-Newtonian fluids with varied flow properties over various geometries that were carried out [23,24].

Porous surfaces and media play a key part in a variety of engineering, industrial, and agricultural activities, including drying processes, geothermal energy, fuel cell equipment, dribbling bed chromatography, oil recovery, and many more. An active tactic to improve thermal performance is the increasing impacts of heat and mass transfer connected to a nanofluid's MHD boundary layer flow by a medium which is porous. In many technological and industrial processes, porous media effectively handle the transmission of fluid velocity and heat. For the flow through a porous media, Darcy provided a classical theory. However, this idea applies to analyses with lower velocity and/or smaller porosity. By including an additional term of square velocity in the momentum eqn, Forchheimer [25] modified the expression of Darcian velocity. Pal and Mondal [26] looked at the flow via non-Darcy porous media, magnetic field impacts, convection, and temperature is dependent on viscosity.
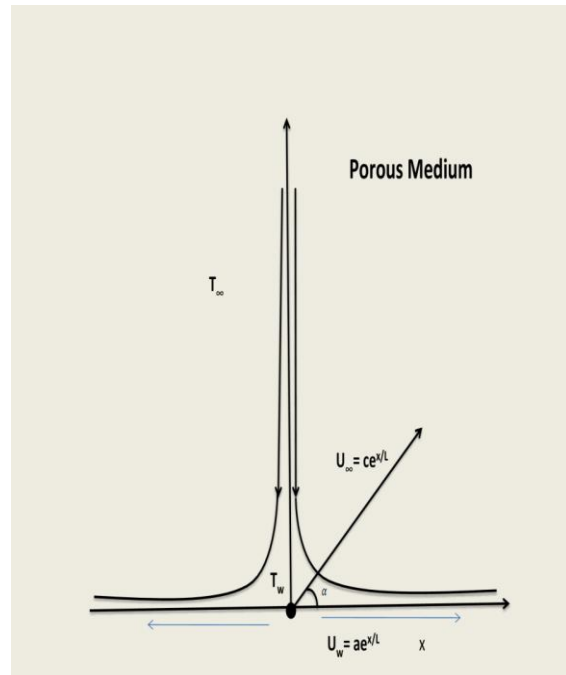
Using the Darcy-Forchheimer theory, Ganesh et al. [27] examined a boundary layer subject to the effects of Ohmic, 2nd-order slip, and water-based nanofluid flowing viscous dissipation via stretched sheet surrounded in a medium that is porous. The purpose of the research is to better comprehend the mechanisms enhancing the heat transmission of Casson nanofluid beyond an exponentially stretched sheet when mixed convection is present. This topic was chosen because it may be employed in a variety of industrial and technical applications, such as gas storage, atomic reactors, heat transmission in cooling and solar devices, motors, and so on.

2. Mathematical Development of the problem

In this investigation, we focused on the steady 2-D flow of an incompressible and viscous Casson fluid close to a stagnation point on an exponentially expanding vertical sheet that is inclined at α an acute angle to the vertical. The x-axis follows a surface that is being stretched in the same direction as the motion is going when the y-axis is at right angles to the surface. The following is a textual" representation of the momentum, energy, and continuity equations [28,29] that control flows of this type:

$$\frac{\partial u}{\partial x} + \frac{\partial v}{\partial y} = 0,$$

$$u\frac{\partial u}{\partial x} + v\frac{\partial u}{\partial y} = \frac{dU_\infty}{dx}U_\infty + \left(1 + \frac{1}{\beta}\right)v\frac{\partial^2 u}{\partial y^2} + F(U_\infty{}^2 - u^2)$$
$$- \frac{B^2}{\rho}\sigma(U_\infty - u)\sin^2(\alpha) + \frac{v}{k^*}(U_\infty - u)$$
$$+ (T - T_\infty)g\beta_T *$$

$$u\frac{\partial T}{\partial x} + v\frac{\partial T}{\partial y} = \dot{\alpha}\frac{\partial^2 T}{\partial y^2} + \frac{\rho_p C_p}{\rho C}\left[D_B\frac{\partial C}{\partial y}\frac{\partial T}{\partial y} + \frac{D_T}{T_\infty}\left(\frac{\partial T}{\partial y}\right)^2\right]$$

$$u\frac{\partial C}{\partial x} + v\frac{\partial C}{\partial y} = \frac{\partial^2 T}{\partial y^2}\frac{D_T}{T_\infty} + \frac{\partial^2 C}{\partial y^2}D_B,$$

$$, u = U_w = ae^{\frac{x}{L}}, v = 0, C = C_w T = T_w \, at \, Y = 0,$$

$$u = U_\infty = ce^{\frac{x}{L}}, , v = 0, C * \to C_\infty T \to T_\infty \, as \, Y \to \infty$$

3. Similarity Transformations

The boundary conditions as well as nonlinear partial differential equations (1)-(5) have been transformed to ODEs using similarity transformations [30, 31].

$$\psi = (2avL)^{\frac{1}{2}}f(\eta)e^{\frac{x}{2L}}, \eta = Y\sqrt{\frac{a}{2vL}e^{\frac{X}{2L}}},$$

$$T = T_0 e^{\frac{X}{2L}}\theta(\eta) + T_\infty, C * = C_0 e^{\frac{x}{2L}} + C_\infty$$

By adding the stream function ψ so that $v = \frac{\partial \psi}{\partial x}$ as well as $u = \frac{\partial \psi}{\partial y}$, G, ψ represent functions of η. The transformed ODEs are as follows after applying the similarity transformations:

$$f'''\left(1 + \frac{1}{\beta}\right) - ff'' - 2f'^2 + M\sin^2(\alpha)f' + 2\epsilon^2 + \gamma(\epsilon - f')$$
$$+ 2\lambda\theta + Fr(\epsilon^2 - f'^2) = 0$$

$$\theta'' + (f\theta' + N_t\theta'' - f'\theta + N_b\theta'\phi')Pr = 0$$

$$\phi'' - Le(f'\phi - f\phi') + \theta''\frac{N_t}{N_b} = 0$$

$$f(0) = 0, f'(0) = 1, \theta(0) = 1, \phi(0) = 1 \, at \, \eta \to 0.$$

$$f'(\infty) = \epsilon, \theta(\infty) = 0, \phi(\infty) = 0 \, at \, \eta \to \infty.$$

The dimensionless parameters are provided as follows:

$$Fr = \frac{C_b}{2\sqrt{k*}}, M = \frac{2\sigma B^2 L}{\rho U_w}, k_p = \frac{2\nu L}{KU_w}, \beta = \frac{\mu_\beta \sqrt{2\pi}}{\tau_y} Pr$$
$$= \frac{\nu}{\gamma}, N_b = \frac{D_B(C_w - C_\infty)(\rho C)_p}{\nu(\rho C)_f}$$

Here Fr indicates Forchheimer number, M is magnetic field parameter, K_p defines porosity parameter, β shows casson fluid parameter, Pr defines Prandtl number, N_b expresses diffusivity parameter, N_t defines thermophoresis parameter

4. Parameters of Empirical Importance

The local Nusselt number, skin friction coefficient, and Sherwood number are defined as follows:
$$Nu_X = \frac{xq_{w\circ}}{\kappa(T_w - T_\infty)}, C_{fX} = \frac{\tau_{w\circ}}{\rho U_w^2(x)}, Sh_x$$
$$= \frac{xq_{m\circ}}{D_B*(C_w - C_\infty)}$$

Here Casson nanofluid's shear stress at the wall's surface is calculated $\tau_{w\circ}$ while $q_{m\circ}$ as well as $q_{w\circ}$ provide the mass and heat fluxes from the wall, respectively. These are the terms listed as

$$\tau_{w\circ} = \mu_0\left(1 + \frac{1}{\beta}\right)\frac{\partial^2 U*}{\partial y^2}, q_{w\circ} = -\varsigma\left(\frac{\partial T}{\partial y}\right)_{y=0}, q_{m\circ}$$
$$= -D_B*\left(\frac{\partial C*}{\partial y}\right)_{y=0}.$$

The non-dimensional forms of the parameters mentioned can be defined by applying similarity transformations as well as dominated boundary conditions.

$$C_{fx}(Re)^{\frac{1}{2}} = \left(1 + \frac{1}{\beta}\right)G''(0)$$
$$Nu_x(Re)^{-\frac{1}{2}} = \left\{\left(-\theta'(\eta)\right) \text{ at } \eta = 0,\right.$$
$$Sh_x(Re)^{-\frac{1}{2}} = \left(-\phi'(\eta)\right) \text{ at } \eta = 0$$

Implementation of the BVP4C Solver: This research has discussed a bvp4c explanatory implementation for the study under consideration. By using similarity transformations, we convert PDEs into ODEs. The process demonstration was provided by Shampine [15].

Step-1
$$f = f(1), f' = f(2), f'' = f(3), \theta = f(4), \theta' = f(5), \phi = f(6), \phi' = f(7)$$
Step-11

$$f' = f(2)$$
$$f'' = f(3)$$
$$f''' = 2(f(2)^2) - f(1)f(3) - 2(\epsilon^2) - 2\lambda f(4) - \gamma(\epsilon - f(2)) - Fr(\epsilon^2 - f(2)^2) + M(f(2) - \epsilon)\sin^2(\alpha))f(2)/(1 + 1/\beta)$$
$$\theta'' = -Pr f(1)f(5) - f(2)f(4) + (Nb)f(5)f(7) + (Nt)f(5)^2)$$
$$\phi'' = -Le f(1)f(7) - f(2)f(6)) + (Nt/Nb)Pr(f(1)f(5)) - f(2)f(4) + (Nb)f(5)f(7) + (Nt)(f(5))^2]$$

Step-111: The boundary conditions change as a consequence of new variables,

$$f_a(1) = 0, f_a(2) = 1, f_a(4) = 1, f_a(6) = 1, f_b(2) = \epsilon, f_b(4) = 0, f_b(6) = 0$$
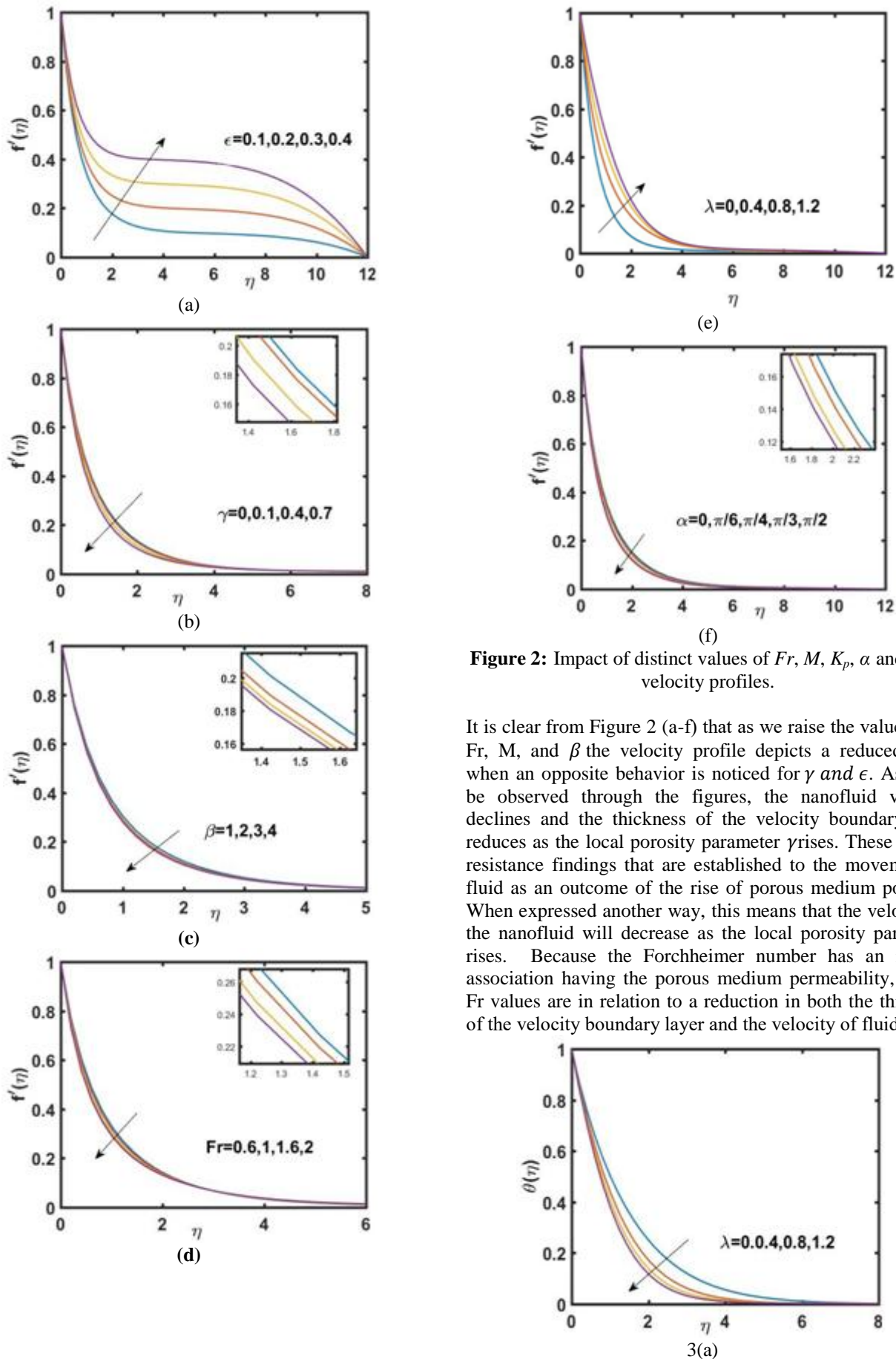
The position at $\eta = 0$ is described by f_a whereas as $\eta \to \infty$ is described by f_b.

Step-IV: The bvp4c solver in MATLAB is utilized for solving a system of first-order equations with boundary conditions. To maintain accuracy, initial assumptions, boundary layer edge position, and step size are changed as necessary.

5. Result and Discussion

In our study, we have investigated heat transfer and the impacts of many increases in physical parameters including γ, Le, Pr, ϵ, N_c, N_t, Fr, and β on temperature $\theta(\eta)$, velocity $f'(\eta)$, and nano-particle concentration profiles $\phi(\eta)$ and findings were shown by figures.

With a few previously published studies, we have compared our results to make sure our assumptions are reasonable and our code is reliable. A comparison of $\theta'(0)$ values for various Pr values in Table -1 in such a way that $K_P = \alpha = N_T = 0 = Fr = M = Le$. We noticed that good agreement between the obtained findings with the findings of Magyari & Keller [33], Sharma & Sood [34], and El-Aziz [35].

Table 1: Comparative $-\theta'(0)$ values for distinct Pr values

| M	Pr	Magyari & Keller (1999)	Sharma & Sood (2022)	El-Aziz (2009)	Present study
0	1	0.954782	0.9548	0.9548	0.9507
0	2	1.4714	1.4715	---------	1,47148
0	3	1.869075	1.8690	1.8691	1.8692
0	5	---------	2.5001	2.500135	2.50013
0	10	3.660379	3.6603	3.66031	3.66037
1	1	--------	0.8615	0.8611	0.86116

(a)

(b)

(c)

(d)

(e)

(f)

Figure 2: Impact of distinct values of Fr, M, K_p, α and β on velocity profiles.

It is clear from Figure 2 (a-f) that as we raise the values of α, Fr, M, and β the velocity profile depicts a reduced trend when an opposite behavior is noticed for γ and ϵ. As could be observed through the figures, the nanofluid velocity declines and the thickness of the velocity boundary layer reduces as the local porosity parameter γ rises. These are the resistance findings that are established to the movement of fluid as an outcome of the rise of porous medium porosity. When expressed another way, this means that the velocity of the nanofluid will decrease as the local porosity parameter rises. Because the Forchheimer number has an inverse association having the porous medium permeability, higher Fr values are in relation to a reduction in both the thickness of the velocity boundary layer and the velocity of fluids".
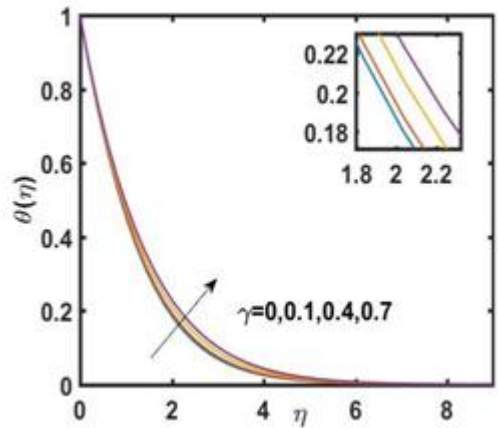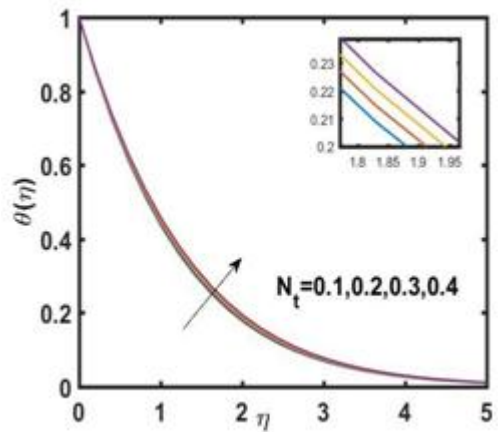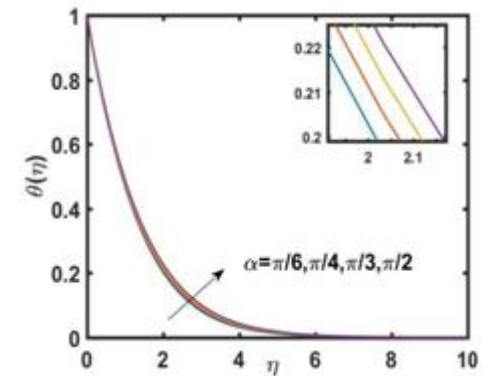

3(a)

3 (b)

3(c)

3(d)

3(e)


3(f)
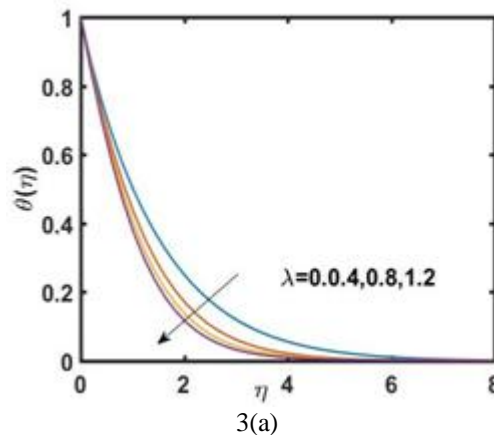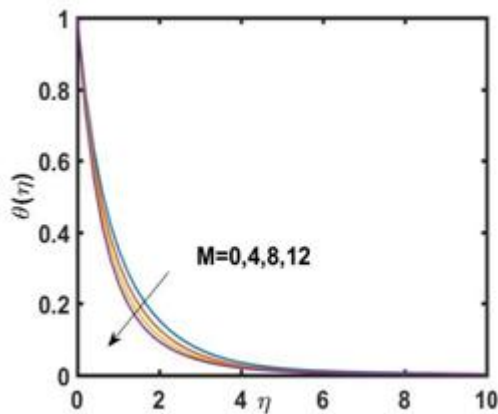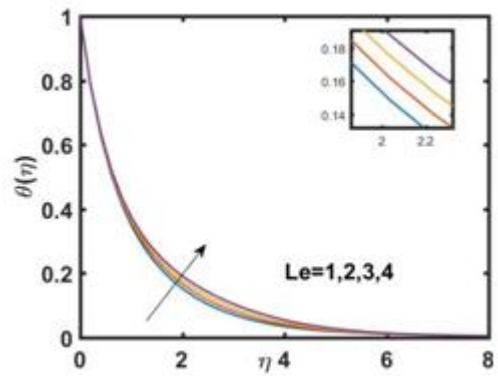
Figure 3: Impact of distinct values of λ ,M, γ., Nt, Le and α on temperature profiles

The variations of important physical parameters on θ (η) are demonstrated in figs. 3(a)-3(f) the effect of mixed convection parameter λ . θ (η) declines while λ elevates as it brings out a temperature difference between the fluid and the locality of the surface. Hence, the thermal boundary layer thickness also decreases. . The porosity of the medium increases as the rate of drag coefficient increases which in turn elevates the temperature profile. As can be seen from the figures, the temperature profile of the nanofluids elevates with increasing rate of γ. There is a declining trend in thermal boundary-layer thickness and temperature for higher value of γ. The fluid which has larger relaxation time shows lesser temperature and the fluid has lesser heat flux relaxation time leads to larger temperature.

4(a)

4 (b)

4(c)

4(d)

4(e)

4(f)

4(g)

4(h)
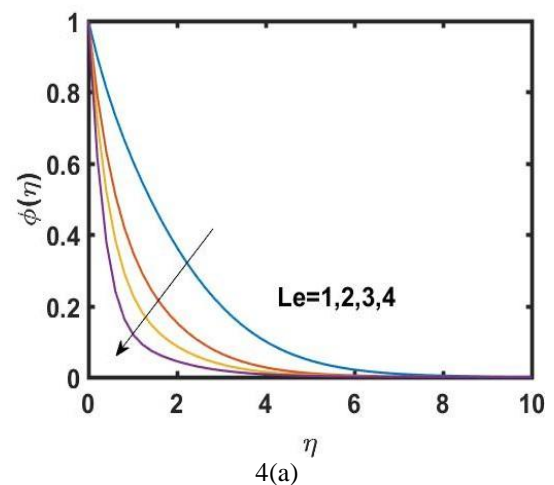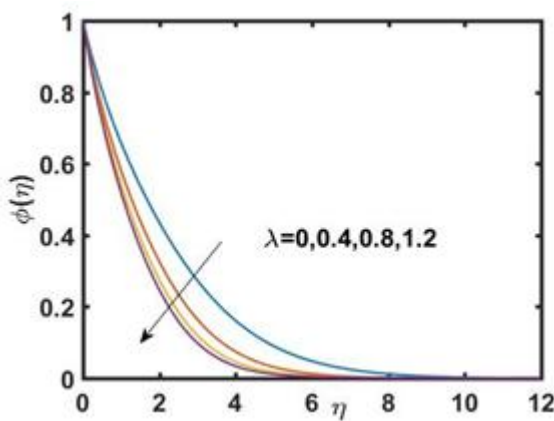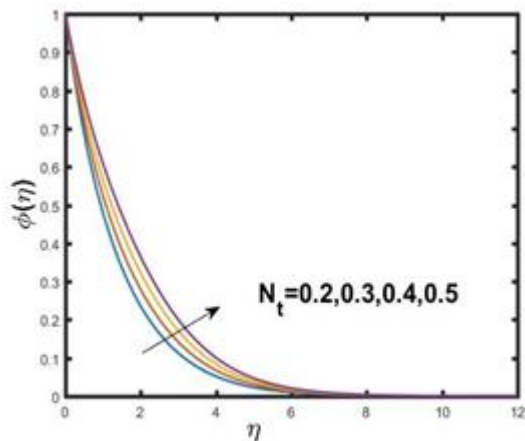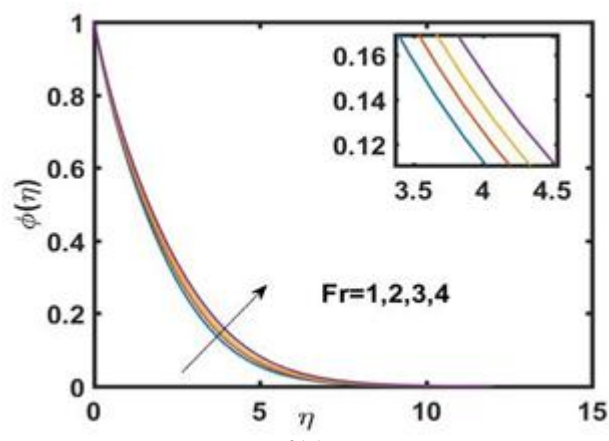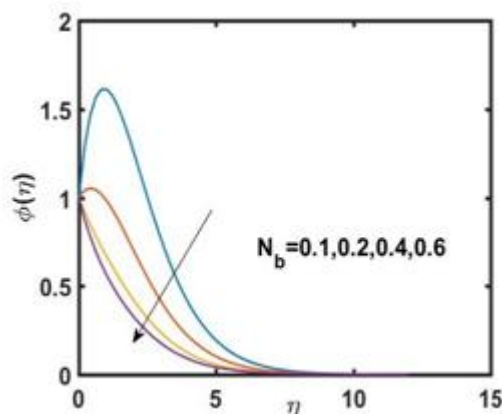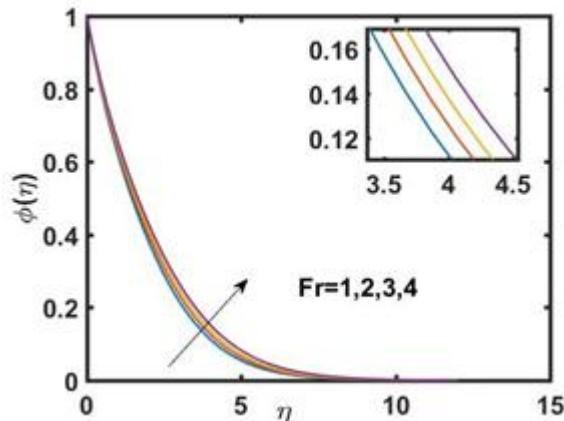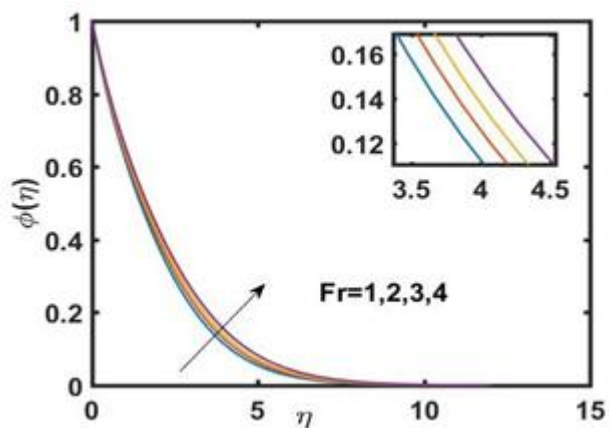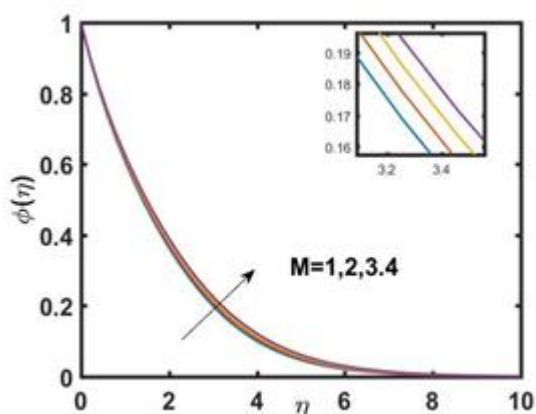
Figure 4: Impact of distinct values of *Fr*, *M*, K_p, *α* and *β* on concentration profiles.

The differences of essential physical parameters on $\phi(\eta)$ are established in the figures. 4(a)-4(h).It is determined that as ϵ rises, the fluid's concentration declines.

A rise in external velocity lowers the fluid concentration, which results in a fall in the volume fraction $\phi(\eta)$ .The rising behavior of $\phi(\eta)$ is caused by an increase in λ. Due to the increase in pressure gradient near the wall, the nanoparticles draw away through the surface. The profile of the volume fraction rises as Fr rises .As the M values rise, the profile of nanoparticle concentration rises. As a result of increased nanoparticle collisions brought on by a fluid flow medium's porosity, the boundary layer's temperature and particle concentration rise.

Table 2: Numerical outcomes for distinct values of significant parameters for the $C_{fx}(Re)^{1/2}$, $Nu_x(Re)^{-1/2}$, $Sh_x\,(Re)^{-1/2}$

β	M	Fr	A	Pr	Le	N_b	N_t	γ	ε	Λ	$C_{fx}\sqrt{(Re)}$	$Nu_x\sqrt{(Re)}^{-1}$	$Sh_x\sqrt{(Re)}^{-1}$
1	1	0.2	90	1	1	0.5	0.5	0.2	0.01	0.2	3.9013	0.71784	0.51004
2											3.1551	0.71045	0.49681
3											2.9252	0.70554	0.48432
4											2.9068	0.70483	0.48051
	0.5										3.4465	0.72931	0.53196
	1.5										4.3602	0.70683	0.49051
	2.0										4.8234	0.6958	0.47449
		0.4									4.1714	0.71387	0.50512
		0.6									4.4053	0.71003	0.5004
		1.0									4.9128	0.70271	0.49154
			30								3.2240	0.73515	0.54401
			45								3.4465	0.72931	0.53196
			60								3.6734	0.72353	0.52061
				0.4							3.7570	0.45761	0.72735
				0.5							3.7945	0.51309	0.68166
				0.7							3.8528	0.60659	0.60108
					0.7						3.9265	0.7448	0.24098
					0.9						3.9217	0.72501	0.42339
					2						3.9123	0.6667	0.85528
						0.4					3.9281	0.74186	0.37012
						0.6					3.9118	0.69285	0.59542
						0.8					3.8958	0.64714	0.70699
							0.6				3.9138	0.70509	0.43039
							0.7				3.9078	0.69365	0.35844
							0.8				3.9019	0.68258	0.28949
								0.3			4.1029	0.7125	0.49767
								0.4			4.2865	0.70813	0.49011
								0.7			4.8417	0.6949	0.47091
									0.1		3.7735	0.72388	0.53595
									0.2		3.4729	0.73706	0.57944
									0.3		3.0574	0.75388	0.62369
										0.3	3.4801	0.72962	0.53160
										0.4	3.0817	0.74071	0.55372
										0.5	2.7150	0.75075	0.57244

Table -2 depicts that C f x (Re)1/2 increases with boosting values of M, Fr, α, Pr and γ whereas it declines with increasing β, Le, Nb, Nt, ϵ and λ . N ux (Re)−1/2 decays with boosting values of β, Fr ,M, , α, Le, Nb, Nt and γ .N ux (Re)−1/2 increases with boosting values of Pr, ϵ and λ .. This could be due to the fact that an enhancement in different parameters such as mixed convection parameter, velocity ratio parameter gives a rise to the temperature difference caused between the sheet and the fluid. It also fastens the rate of heat scattering in the vicinity of the sheet because of the increase in the external velocity.. It can be seen a variation in the Sherwood number for different values of ϵ , λ , Le , Nb . $Sh_x\,(Re)^{-1/2}$ decreases slightly with boosting values of β, Fr ,M, , α, Nt , Pr and γ .

6. Conclusion

This research represents a numerical evaluation of the Casson nanofluid steady-state boundary layer flow and transfer of the heat in a medium that is porous lying on an exponentially stretched surface. Velocity distribution has a dropping pattern with increasing Casson nanofluid parameter (β),Darcy-Forchheimer parameter Fr, porosity parameter(γ), inclination angle (α), and magnetic field (M) values, whereas temperature and concentration profiles exhibit a rising trend with the same parameters. Nt, Nb, and Le rise, increasing the temperature profile. The Pr represented as the Prandtl number is a declining function of both temperature and the

thermal boundary layer. When a rise in ϵ, the velocity profile $f'(\eta)$ rises and the temperature field $\theta(\eta)$ falls.

The skin friction coefficient shows a significant correlation with the variables γ, M, Fr, and α, and is inversely associated with β. Growing values of γ, M, Fr, α, and β result in a decline in the local Nusselt number. The Sherwood number drops with the rise in the values of" γ, M, β, Fr, Pr, Nb, and α, while it boosts with Le and Nb.

References

[1] Mahapatra TR, Gupta AS. Heat transfer in stagnation-point flow towards a stretching sheet. Heat and Mass transfer. 2002 Jun;38(6):517-21.

[2] Nazar R, Amin N, Filip D, Pop I. Stagnation point flow of a micropolar fluid towards a stretching sheet. International Journal of Non-Linear Mechanics. 2004 Sep 1;39(7):1227-35.

[3] Sadeghy K, Hajibeygi H, Taghavi SM. Stagnation-point flow of upper-convected Maxwell fluids. International journal of non-linear mechanics. 2006 Dec 1;41(10):1242-7.

[4] Ishak A, Nazar R, Arifin NM, Pop I. Mixed convection of the stagnation-point flow towards a stretching vertical permeable sheet. Malaysian Journal of Mathematical Sciences. 2007;1(2):217-26.

[5] Ishak A, Nazar R, Bachok N, Pop I. MHD mixed

convection flow near the stagnation-point on a vertical permeable surface. Physica A: Statistical Mechanics and its Applications. 2010 ;389(1):40-6.

[6] Tamim H, Dinarvand S, Hosseini R, Khalili S, Pop I. Unsteady mixed convection flow of a nanofluid near orthogonal stagnation point on a vertical permeable surface. Proceedings of the Institution of Mechanical Engineers, Part E: Journal of Process Mechanical Engineering. 2014; 228(3):226-37.

[7] Jamaludin A, Nazar R, Pop I. Three-dimensional mixed convection stagnation-point flow over a permeable vertical stretching/shrinking surface with a velocity slip. Chinese Journal of Physics. 2017; 55(5):1865-82.

[8] Ahmad Dar A, Elangovan K. Influence of an inclined magnetic field and rotation on the peristaltic flow of a micropolar fluid in an inclined channel. New Journal of Science. 2016:2016:14.

[9] Ferraro V C ,Plumpton C. Introduction to magneto-fluid mechanics. Second edition. United States: N. p., 1966. Web.

[10] Stud VK, Sephon GS, Mishra RK. Pumping action on blood flow by a magnetic field. Bulletin of mathematical biology.1977;39(3):385-90.

[11] Uddin MJ, Rasel SK, Rahman MM, Vajravelu K. Natural convective heat transfer in a nanofluid-filled square vessel having a wavy upper surface in the presence of a magnetic field.Thermal Science and Engineering Progress. 2020; 19:100660.

[12] Ibrahim W, Makinde OD. Magnetohydrodynamic stagnation point flow of a power-law nanofluid towards a convectively heated stretching sheet with slip. Proceedings of the Institution of Mechanical Engineers, Part E: Journal of Process Mechanical Engineering. 2016 ;230(5):345-54.

[13] Khan WA, Makinde OD, Khan ZH. Non-aligned MHD stagnation point flow of variable viscosity nanofluids past a stretching sheet with radiative heat. International Journal of Heat and Mass Transfer. 2016;96:525-34.

[14] Ibrahim W, Makinde OD. Magnetohydrodynamic stagnation point flow and heat transfer of Casson nanofluid past a stretching sheet with slip and convective boundary condition. Journal of Aerospace Engineering. 2016; 29(2):04015037.

[15] Makinde OD, Khan WA, Khan ZH. Stagnation point flow of MHD chemically reacting nanofluid over a stretching convective surface with slip and radiative heat. Proceedings of the Institution of Mechanical Engineers, Part E: Journal of Process Mechanical Engineering. 2017 ;231(4):695-703.

[16] Makinde OD, Khan WA, Khan ZH. Buoyancy effects on MHD stagnation point flow and heat transfer of a nanofluid past a convectively heated stretching/shrinking sheet. International journal of heat and mass transfer. 2013 ;62:526-33.

[17] Huang JS, Tsai R, Huang KH, Huang CH. Thermal-diffusion and diffusion-thermo effects on natural convection along an inclined stretching surface in a porous medium with chemical reaction. Chemical Engineering Communications. 2010 ;198(4):453-73.

[18] Qasim M, Hayat T, Obaidat S. Radiation effect on the mixed convection flow of a viscoelastic fluid along an inclined stretching sheet. Zeitschrift für Naturforschung A. 2012 ;67(3-4):195-202.

[19] Sravanthi CS. Homotopy analysis solution of MHD slip flow past an exponentially stretching inclined sheet with Soret-Dufour effects. Journal of the Nigerian Mathematical Society. 2016 ;35(1):208-26.

[20] Abo-Eldahab EM, El Aziz MA. Blowing/suction effect on hydromagnetic heat transfer by mixed convection from an inclined continuously stretching surface with internal heat generation/absorption. International Journal of Thermal Sciences. 2004 ;43(7):709-19.

[21] Lok YY, Amin N, Campean D, Pop I. Steady mixed convection flow of a micropolar fluid near the stagnation point on a vertical surface. International Journal of Numerical Methods for Heat & Fluid Flow. 2005 Oct 1;15(7):654-70.

[22] Seshadri R, Sreeshylan N, Nath G. Unsteady mixed convection flow in the stagnation region of a heated vertical plate due to impulsive motion. International Journal of Heat and Mass Transfer. 2002 Mar 1;45(6):1345-52.

[23] Ishak A, Nazar R, Bachok N, Pop I. MHD mixed convection flow near the stagnation-point on a vertical permeable surface. Physica A: Statistical Mechanics and its Applications. 2010 Jan 1;389(1):40-6.

[24] Kumar D, Sinha S, Sharma A, Agrawal P, Kumar Dadheech P. Numerical study of chemical reaction and heat transfer of MHD slip flow with Joule heating and Soret–Dufour effect over an exponentially stretching sheet. Heat Transfer. 2022 ;51(2):1939-63.

[25] Forchheimer, P.: Wasserbewegung durch boden. Zeit. des Ver. deut. Ing. 1901; 45: 1782–1788.

[26] Pal D, Mondal H. Hydromagnetic convective diffusion of species in Darcy–Forchheimer porous medium with non-uniform heat source/sink and variable viscosity. International Communications in Heat and Mass Transfer. 2012; 39(7):913-7.

[27] Ganesh NV, Hakeem AA, Ganga B. Darcy–Forchheimer flow of hydromagnetic nanofluid over a stretching/shrinking sheet in a thermally stratified porous medium with second order slip, viscous and Ohmic dissipations effects. Ain Shams Engineering Journal. 2018 ;9(4):939-51.

[28] Mustafa M, Hayat T, Pop I, Aziz A. Unsteady boundary layer flow of a Casson fluid due to an impulsively started moving flat plate. Heat Transfer-Asian Resc 2011; 40(6):563–76.

[29] Azhar E, Iqbal Z, Ijaz S, Maraj EN. Numerical approach for stagnation point flow of Sutterby fluid impinging to Cattaneo–Christov heat flux model. Pramana. 2018 Nov;91:1-7.

[30] Seini YI, Makinde OD. MHD boundary layer flow due to exponential stretching surface with radiation and chemical reaction. Mathematical Problems in Engineering. 2013 Jan 1;2013.

[31] Rohni AM, Ahmad S, Ismail AI, Pop I. Boundary layer flow and heat transfer over an exponentially shrinking vertical sheet with suction. International Journal of Thermal Sciences. 2013 Feb 1;64:264-72.

[32] El-Aziz MA. Viscous dissipation effect on mixed convection flow of a micropolar fluid over an exponentially stretching sheet. Canadian Journal of Physics. 2009;87(4).

[33] Sharma, D., Sood, S.: Effect of inclined magnetic field on flow of Williamson nanofluid over an exponentially stretching surface in Darcy-Forchheimer Model. Z. Angew. Math. Mech. e202100425 2022..

[34] Magyari E, Keller B. Heat and mass transfer in the boundary layers on an exponentially stretching continuous surface. Journal of Physics D: Applied Physics. 1999 Mar 7;32(5):577.

[35] Shampine LF, Kierzenka J, Reichelt MW. Solving boundary value problems for ordinary differential equations in MATLAB with bvp4c. Tutorial notes. 2000 Oct 26;2000:1-27.